Gel-to-Solid Transition in Polyethylene from the Viewpoint of the Crystallization Process

Pavel Pakhomov,[†] Svetlana Khizhnyak,[†] Hans Reuter,[‡] Manfred Lechner,[‡] and Alexandre Tshmel*[,§]

Physico-Chemistry Department, Tver' State University, 170002 Tver', Russia, University Osnabrueck, Barbara Strasse 7, D-49069 Osnabrueck, Germany, and Ioffe Physico-Technical Institute, Russian Academy of Sciences, 194021 St. Petersburg, Russia

Received February 2, 2003; Revised Manuscript Received May 2, 2003

ABSTRACT: The crystalline phase in gels and solid gel-derived samples of ultrahigh molecular weight polyethylene was studied using the infrared spectroscopy, low-frequency Raman spectroscopy and wide-angle X-ray scattering methods. The spectroscopic data evidence the presence in gels of tiny crystallites whose thickness (3−5 nm) depends on the sort of the solvent used and it is insensitive neither to the concentration of the diluted solution, nor to the molecular weight of the polymer. After removal of the solvent, there appear crystalline clusters composed of closely attached folded platelets. The total thickness of these stacked entities is about 10−20 nm while their transverse size reaches ∼50 nm. In addition, the crystalline domains in the gelled material exhibit a kind of mosaic structure which is much more pronounced in solid xerogels than in wet gels.

Introduction

A formal sign that helps one to distinguish a gelled substance from the liquid is the gel's ability to maintain its shape. In polymer gels, this ability is conditioned by the macromolecular network permeating the solvent. The strength and connectedness of the spatial network determine the properties not only of the gel itself but also the performance of gel-derived products such as fibers, porous materials, and membranes. The advantage of the polymeric gels issues from the properties of the network, which is tenuous and stable at the same time. Tiny crystalline entities serve as entanglements.[1,2] Therefore, the nucleation of these crystalline "islands" in a dissolved polymer is the first step to the formation of the gel substance. In previous works[3,4] we reported the infrared (IR) data evidencing the presence of tiny (nanoscopic) crystallites in a highly diluted solution of the ultrahigh molecular weight polyethylene (UHMWPE) at polymer concentrations below a critical level of gelling. The crystallite size along the chain orientation was evaluated from low-frequency Raman spectroscopy.[4,5] These results supported the model of Keller[2] where the gel network in semicrystalline polymer was considered as composed of folded-chain platelets immersed in the solvent and connected to each other by flexible links. However, up to now there is a very limited information about the structure of the primary crystallites including their size distribution and crystalline perfection.

In the present work, vibrational spectroscopy and wide-angle X-ray scattering (WAXS) techniques were used to trace the transformation of the gel substance to solid polymer as a result of the removal of the solvent.

* To whom correspondence should be addressed. Fax: +7-812-2478924. E-mail: chmel@mail.ioffe.ru.
[†] Tver' State University.
[‡] University Osnabrueck.
[§] Russian Academy of Sciences.

Samples and Techniques

The experiments were performed on a set of samples made of ultrahigh molecular weight polyethylene (UHMWPE) with the molecular weight (M_w) in the range from 1.6×10^6 to 14.2×10^6. The values of M_w were determined from measurements of the specific viscosity.

The PE solutions were prepared in a thermostat. Paraffin oil, Decalin, and *p*-xylene were used as solvents. The suspensions of the polymeric powder were slowly heated from 20 to 140 °C (when using *p*-xylene) or to 180 °C (when using paraffin oil and Decalin) with intensive stirring. To suppress the Weissenberg effect, stirring elements of brushlike shape were used. The concentrations of the suspensions were 0.01 to 2.5 wt %.

The polymer particles exhibited swelling at the temperature from 90° to 110 °C and then dissolved at 110−115 °C. The hot UHMWPE solution (140/180 °C) was poured into a glass Petri plate. Rapid cooling resulted in gel formation which was concluded from the rheological tests performed at 60 °C using a rotary viscometer Carri-Med CSL 100.

To obtain solid samples (xerogels), the gels were dried and shaped to films of ∼200 μm thickness. The wet preforms derived from x-xylene and Decalin remained a few days under room conditions to provide a spontaneous yield of the volatile solvent. The residual solvent was controlled with the help of a Perkin-Elmer calorimeter model DSC-2. To remove the low-volatile paraffin oil from the gel, the sample was repeatedly squeezed between sheets of filter paper in a hand press.

The IR spectra were measured with a Fourier spectrometer Bruker model Equinox 55.

The Raman spectra were recorded with a triple monochromator DILOR XY 800 using a Spectra Physics 100 mW NdYVO4 laser.

The WAXS experiments were performed on a STADI P STOE & CIE X-ray diffractometer using a monochromatic $\lambda = 1.54$ Å radiation (λ is the wavelength).

Experimental Results

IR Spectroscopy. At the stage of gel formation the morphology of substance is characterized by the presence of a network composed of flexible chains with entanglements of any kind. A cross-linked system appears when a UHMWPE concentration in solution (c_s) is higher than a certain critical limit (c_s*). At this critical

10.1021/ma034139g CCC: $25.00
Published on Web 06/06/2003

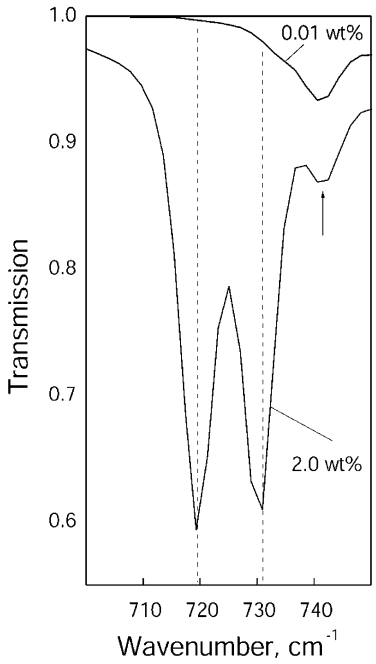

Figure 1. IR doublet at 720 and 731 cm^{-1} in the transmission spectra of UHMWPE gels prepared from solutions with polymer concentrations 2.0 and 0.01 wt %. In the latter case the "crystalline" 731 cm^{-1} band is hardly seen on the shoulder of the feature at 742 cm^{-1} (arrow) belonging to a solvent. $M_w = 2.4 \times 10^6$ without a commonly linked network.

Table 1. Minimum Concentration of UHMWPE Solution Ensuring the Formation of a Gel Network

M_w	solvent	c_s*
2.4×10^6	*p*-xylene	0.5
2.4×10^6	Decalin	0.5
7.5×10^6	Decalin	0.3
14.2×10^6	Decalin	0.1

concentration we observed a sharp increase of the shear modulus of the polymeric system (approximately from 10^1 to 10^4-10^5 Pa) which evidenced the gel formation. The value c_s* depends noticeably on the M_w of polymer (Table 1).

To find a structural response to the increased connectedness of the substance, the IR spectra of the gels prepared from solutions with concentration both higher and lower than c_s* were recorded in the frequency range of a doublet at 720 and 731 cm^{-1} (Figure 1). The band at 720** cm^{-1} is due to the trans sequence in both crystalline and amorphous domains while the band at 731 cm^{-1} represents the trans segments occurring in the crystalline regions only. The doublet appeared in the IR spectra at concentrations as low as 0.01 wt % though the reliable band intensities could be measured only at $c_s \sim 0.1$ wt % or higher. One can see that this is lower than the critical value c_s* (Table 1). Consequently, the "islands" of the orthorhombic crystalline modification occur even in the solution.

For determination of the degree of crystallinity, κ, we used an empirical relation:

$$\kappa = (\alpha_{731}/k) \times 100\% \qquad (1)$$

where α_{731} is the Lambert−Beer coefficient of the 731 cm^{-1} band; $k = 550$ cm^{-1} [3]. The κ vs c_s plots for different UHMWPE and different solvents are shown in Figure 2. The plateau in the range of the critical concentration of dissolved polymer (c_s = 0.2−0.5%) is due to the increased polymer mobility of macromolecules, thus hindering the chain folding process which, in its turn, impedes the nucleation of new primary crystals. This situation is traced in both κ vs c_s dependences shown in Figure 2.

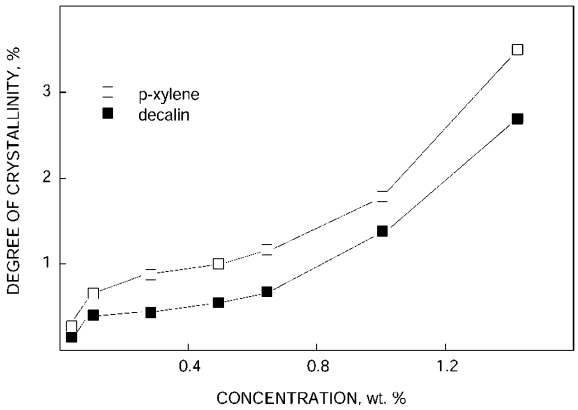

Figure 2. Degree of crystallinity vs solution concentration.

In addition, one can note that the degree of crystallinity of Decalin-derived gels is lower than the crystallinity of the samples gelled in *p*-xylene throughout the measured concentration range. This may be caused by the difference in either the amount of crystallites or their size. The IR experiment gives poor information on the crystal dimension since the doublet at 720 and 731 cm^{-1} occurs in the presence in a crystal site of, at least, two chain segments each of which includes more than seven trans-conformers.[6] The length of such regular sequence is a lower estimate for the crystal size in gels that is about 1 nm. More exact information about the dimensions of crystalline regions is available from Raman and WAXS measurements.

Low-Frequency Raman Spectroscopy. In semicrystalline polymers with all-trans sequences, the longitudinal acoustic vibrations propagate along these regular segments like along the elastic rods. The chain vibrations of this kind are called longitudinal acoustic modes (LAM), and these modes produce specific bands in the low-frequency Raman spectra. It should be stressed that the linearity of the chain is a necessary condition of the propagation of LAM since there appear to be transverse oscillations in chain-breaking points. As a result, the redistribution of the vibrational energy in "defects of linearity" leads to the effective attenuation of the longitudinal mode. Length of the all-trans sequence (l) between chain-ends and/or defects (gauche-conformers, points of branching) is related with the LAM frequency (ω_l) as

$$l = (2c\nu_l)^{-1} \times (E/\rho)^{1/2} \qquad (2)$$

where c is the speed of light; ρ is the density, and E is the Young's modulus along the straight chain axis. The frequency of the maximum of the LAM band allows one to calculate the most probable length of the straight segments (l_{pro}); as a rule, this is close to the average crystal size in the chain direction (l_c).[7]

Since each all-trans stem of a given length has its specific LAM frequency, the LAM band as a whole reflects the contribution of the straight chain segments (SCS) of different lengths to the Raman intensity, or in other words, the average number SCS length distribution. However, owing to the dependence of the distribution function $F(l)$ not only on the number of vibrating

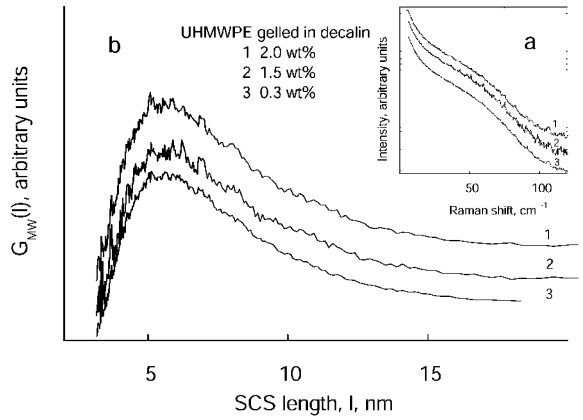

Figure 3. Low-frequency Raman spectra in the range of the LAM bands (a) and calculated from them SCS length distributions (b) in the UHMWPE gelled in Decalin solutions of different concentrations.

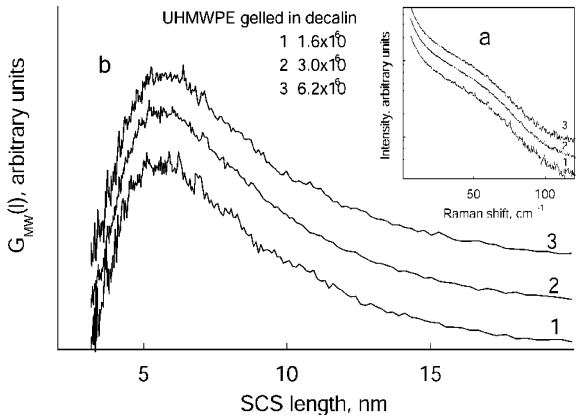

Figure 4. Raman spectra in the range of the LAM bands (a) and the SCS length distributions (b) in the gelled solutions of UHMWPE of different M_w.

SCS but also on the scattering efficiency of light and the population of vibrational energy levels, the original Raman spectrum is poor representative for aims of quantitative estimations, and $F(l)$ must be computed using a procedure based on the relation:[7]

$$F(l) \propto [1 - \exp(-hc\omega/kT)]\omega^2 I(\omega) \qquad (3)$$

Here h is Planck's constant, k is Boltzmann's constant, T is the absolute temperature, and $I(\omega)$ is the Raman intensity. The expression $[1 - \exp(-hc\omega/kT)]$ characterizes the Boltzmann population of vibrational energy levels. The value of the distribution function calculated at given l is proportional to the fraction amount of the SCS with the length equal to l.

The relative weight fraction of ordered sequences of length l is given by the function $G_{MW}(l)$:

$$G_{MW}(l) \propto F(l) \times l \qquad (4)$$

To exclude the contribution of the Rayleigh scattering, a background of the LAM spectrum in the vicinity of the of central line was approximated with the Lorentz function which is very applicable for this procedure in the case of oriented polymers.[8] The difference between the experimental spectrum and the approximating Lorentzian was taken as the effective intensity $I(\omega)$ in eq 3.

Figure 3 shows the LAM spectra of gels prepared in solutions of three different concentrations. The SCS length distributions calculated from these spectra are given in Figure 4. One can see that the profiles of all the distributions are very similar (the same result was obtained with two other solvents—not presented). On the other hand, the IR data (Figure 2) demonstrate the increase of the crystallinity with the concentration increase. Hence, we conclude that this growth of the crystallinity is due to the growth of the number of crystallites but not their size.

We also failed to detect the dependence of the distribution function $G_{MW}(l)$ on the M_w of the original polymer (Figure 4). One could expect this result bearing in mind that the crystal size is determined by the thermodynamic conditions of the folding process which, in its turn, is independent of the molecular characteristics of the polymer of $M_w > 10^3$.[9] However, we have revealed that the SCS length distribution is sensitive to the sort of solution. It is seen in Figure 5 that the crystallites

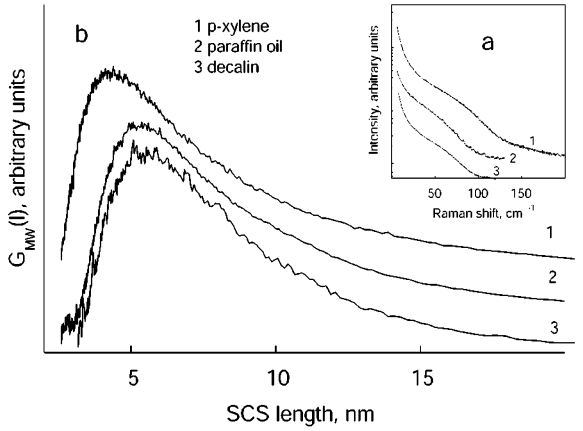

Figure 5. Raman spectra in the range of the LAM bands (a) and the SCS length distributions (b) in the UHMWPE gelled in solutions of different kind.

formed in Decalin and paraffin oil are noticeably larger than those nucleated in a polymer gelled in *p*-xylene ($l_c \approx 51$ Å against 37 Å, respectively).

This result points out that the difference in the degree of crystallinity between the samples derived from Decalin and *p*-xylene observed in the IR experiment is due to smaller size of the crystallites in the latter case. We explain the effect of solvent by the difference in the boiling temperatures between *p*-xylene (138 °C) on one hand, and Decalin (186 °C) and paraffin oil (about 360 °C) on the other hand. In the case of *p*-xylene, the crystallization process runs close to the boiling temperature of solvent; the strong convection hinders the growth of crystallites.

The SCS length distributions change significantly after the removal of solvent from gels. The Raman spectra and the calculated SCS length distributions in solvent-free xerogels are shown in Figure 6. An asymmetry of the SCS length distribution with a long $l > l_c$ tail indicates the imperfect geometry of the basal planes in crystallites. In the solid samples the function $G_{MW}(l)$ is bimodal, and the value l_c is smaller than that in the wet gels (Table 2). The effect is more pronounced in more concentrated solution. The LAM method does not distinguish between the SCS involved in crystalline entities and the individual all-trans sequences that link statistic balls or situated within balls. Therefore, the most probable SCS length determined from the position of the main maximum of the function $G_{WM}(l)$ is, in fact, higher than its true value. The divergence between the

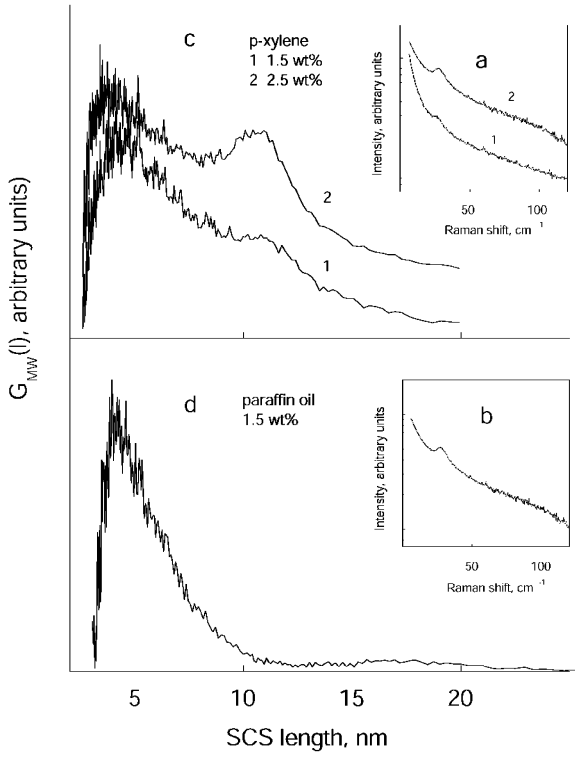

Figure 6. Raman spectra in the range of the LAM bands (a, b) and the SCS length distributions in the xerogels prepared in *p*-xylene (c) and paraffin oil (d).

Table 2. Thickness of Lamellar Crystals (Å) in Solvent-Free Xerogels as Calculated from the Raman Data

source	primary crystallites[a]	secondary crystallites	M_w^{SC}/M_w^{PC} [b]
p-xylene	47 ± 0.2	110 ± 0.2	0.40
paraffin oil	49 ± 0.2	170 ± 1	0.05

[a] Succeeded to gel. [b] SC = secondary crystallites; PC = primary crystallites.

l_{pro} and l_c must be more significant in lower perfect crystallites. Hence, one can interpret the shift of the $G_{WM}(l)$ maximum to shorter lengths as due to smoothening of the crystal surface as a result of coiling the portions of the SCS that quit the crystallite cores normal to their surface. Second, a weak-amplitude peaks situated at ~120 and 170 Å in the spectra of the samples prepared in, respectively, *p*-xylene and paraffin oil demonstrate the formation of some quantity of SCS whose lengths are a few times more than the longitudinal size of the crystallites. In view of the uniformity of the thermal prehistory of the material, one cannot ascribe these "long" ordered stems to the SCS in crystallites of other thickness. On the other hand, the arising of a well-pronounced extra peak in the SCS length distribution points out the existence of a particular dimension in the structure.

Such "quantum" dimensions can arise as a result of the penetration of some SCS into adjacent crystallites with formation of regular sequences similar to taut-tie molecules in oriented structures. In this case, a peak corresponding to stems linking neighboring crystals must be situated at $l = l_c \times n + \delta$, where δ is the average length of the intercrystallite spacers. We suppose that the peak belonging to the SCS involved in two ($n = 2$; $l_c = 43$ Å) closely arranged crystallites ($l = 43 \times 2 + \delta$)

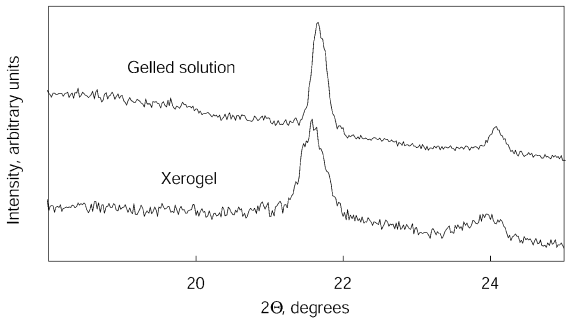

Figure 7. WAXS profile from gelled solution of UHMWPE in paraffin oil (a) and xerogel (b) in the range of crystalline components [110] and [200].

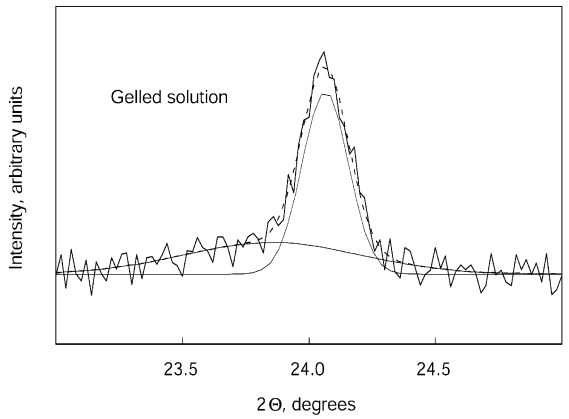

Figure 8. Deconvoluted WAXS peak [200] from gelled solution of UHMWPE in paraffin oil.

is overlapped by the main dome. The well-resolved isolated peak at170 Å is due to the SCS passing through three ($n = 3$) stacked folded crystals: $170 = 43 \times 3 + 2\delta$.

WAXS. The experimental WAXS curves from gel and solvent-free xerogel in the range of the equatorial diffraction peaks [110] and [200] are shown in Figure 7. One can distinguish an asymmetry of the crystalline components which is more pronounced in a solid sample.

The peak asymmetry is caused by the deviation of a certain number of unit cells from their canonical orthorhombic configuration in view of the presence of defect sites in crystallites or the imperfection of some crystallites in whole.[10] The difference in the manifestation of the effect between two detected equatorial peaks is caused by the difference in the response of planes (110) and (200) to the crystal deformation. The low-angle character of the skew in the scattering profile evidences the presence of abnormally large interchain spacings in defect sites.[11] To estimate the specific contributions of the unresolved peaks to asymmetric X-ray scattering curves, we applied a routine deconvolution procedure (Figures 8 and 9). The experimental diffraction peaks [200] in the WAXS spectra of gel solution and solid xerogel were corrected for the background scattering, and then each corrected curve was approximated by two Gaussian components. The resulted profiles demonstrate good fitting to the experimental curves. The calculated parameters of the components are given in Table 3.

Angular positions of the maxima of the crystalline components are determined by the cell parameters a_i

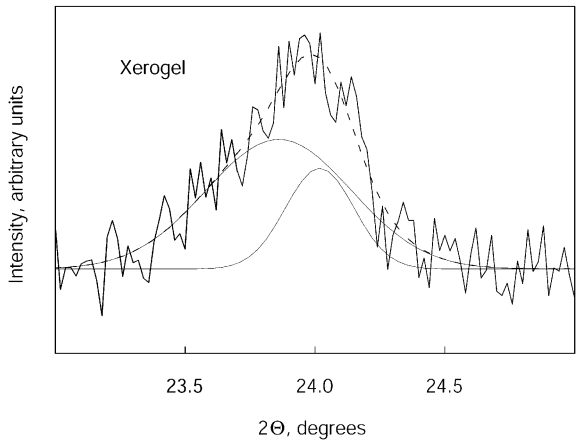

Figure 9. Deconvoluted WAXS peak [200] from xerogel derived from paraffin oil.

Table 3. Angular Position and Half-Width of the Diffraction Peak from Planes (200) in UHMWPE Gels (in deg)

sample	$2\Theta_1$	$2\Delta\Theta_1$	$2\Theta_2$	$2\Delta\Theta_2$
gel solution	24.06 ± 0.01	0.69 ± 0.02	23.85 ± 0.05	0.18 ± 0.02
solid xerogel	24.03 ± 0.02	0.52 ± 0.03	23.84 ± 0.04	0.27 ± 0.03

Table 4. Some Dimensional Characteristics of the Crystalline Phase in UHMWPE Gels Prepared in Paraffin Oil (Å)

sample	a_1	a_2	L_1	L_2
gel solution	7.39 ± 0.01	7.43 ± 0.02	470 ± 20	120 ± 10
solid xerogel	7.40 ± 0.01	7.44 ± 0.01	310 ± 30	160 ± 20

(here i is the conventional number of the component, see Figure 2) in accordance with the basic relation:

$$2a_i = m\lambda/\sin\theta_{[200]}^{(i)} \quad (5)$$

(Here m is the diffraction order; in our case $m = 2$).

The values a_i found from eq 4 are collected in Table 4 together with the transverse crystallite dimensions (L_c^i) calculated using the Debye−Scherrer formula:

$$L_c^{\,i} = K\lambda/(\beta\cos\theta_{[200]}^{(i)}) \quad (6)$$

where $K = 0.94$ is the constant and β is the peak half-width measured in radians. As ascribing to every Gaussian component a specific value of L_c^i, we imply indirectly that two sorts of unit cells belong to crystalline domains differing in transverse size.

Discussion

The main diffraction peak [200] ($i = 1$) at $2\theta \approx 24°$ in both convoluted WAXS spectra is obviously corresponded to the unit cells whose parameter a_1 is close to the value 7,41Å characteristic for orthorhombic unit cells.[12] The peak at lower 2θ ($i = 2$) could be regarded as due to the contribution of "defect" cells with dimensions a_2 other than a_1. The areas under the Gaussian components correspond to the weight fractions of the unit cells of these two sorts.

When comparing the deconvoluted scattering curves of the gelled solution and solid xerogel, one can see that despite the intensity perturbation in the X-ray pattern as a result of the gel-to-solid transition, the positions of the extra peaks related to distorted cells remain the same. We conclude that in both liquid and solid gel phases there are structural defects due to the scattering on the (200) planes in particular. Among possible steric defects capable of affecting the unit cell parameters, Davis and co-workers[9] called those that originate from the fold interaction, from the difference in fold planes, and from the crystal site distortion in molecular domains of all kinds. We suppose that in the case of ill-ordered structure, the defects of fold packing in crystallites are the prevailing cause of the bimodal cell dimension distribution.

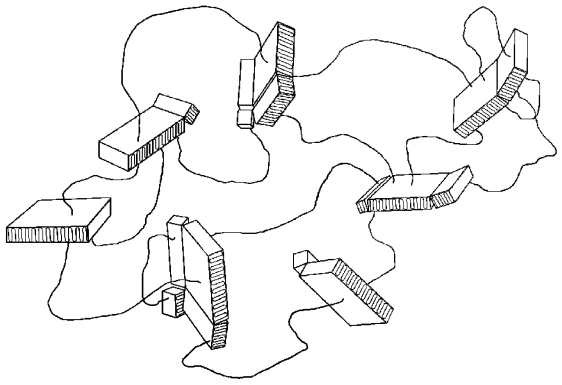

Figure 10. Schematic representation of the Keller model[1] modified in accordance with the actual WAXS data.

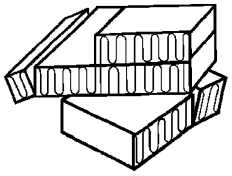

Figure 11. Stacked crystalline platelets formed as a result of the gel-to-solid transformation.

In the framework of the Keller model,[2] this means that the crystalline platelets imbedded in the gelled substance have substantial defects in the fold packing which affect the regular diffraction pattern (Figure 10). The defects of this kind one should expect in mosaic crystallites, in particular, those that cracked with incomplete separation of broken parts. The disturbance of regular folding along the adjacent (connected) edges of the crystallite parts must cause the local tensile strain with gaining the diffraction intensity at $2\theta < 2\theta_1$.

As regards the longitudinal crystal size, this characteristic remains unchanged since the solvent was removed from the gel without a heat treatment. However, as a result of the gel-to-solid transformation, the structure becomes much more compacted. Some lamellar crystallites enter in close contact, forming a kind of "sandwich" with uniformly oriented (complanar) fold planes (Figure 11). These stacked platelets become linked by the intercrystallite $l > 2l_c$ regular stems that produce an individual peak in the SCS length distribution (Figure 6).

A similar effect of the fold doubling was first observed by Keller and co-workers[13−15] in their experiments on annealing PE single crystals and solution-crystallized polyamides. A "quantum" increase of the crystal size was explained by penetration of folds from one lamella into adjacent lamella, resulting in chain sliding through the interface. Rastogi and co-workers[16] also applied this model in order to interpret the experiments on melting the gel-derived PE samples. Dreyfuss and Keller[14]

stressed that the folds in the intermediate state (i.e., those of $l_c < l < 2l_c$) are unstable in principle; therefore, the doubling compensates the "missing" SCS within the defect crystallites. The thermodynamic driving force that causes the chains to slide is related to the necessity to minimize the surface free energy under specific conditions.[13]

Conclusions

The primary crystallites existing in wet polyethylene gel could be regarded as precursors of the crystalline structure of xerogels. The basal planes of these crystallites are quite imperfect. As a result of the gel-to-solid transformation, a great part of the unfolded SCS extending from the crystallite cores to the interface zones become coiled, thus smoothing the fold surfaces; at the same time, clusters consisting of two to three complanar lamellar crystals appear in compacted xerogels. The WAXS data evidence a mosaic structure of crystallites in the UHMWPE gel and xerogel. The effect is gained by the cracking of the primary crystallites at the stage of gel-to-solid transformation.

Acknowledgment. This work was supported by the DAAD (Germany).

References and Notes

(1) De Gennes, P.-G. *Scaling Concepts in Polymer Physics*; Cornell University Press: Ithaca, NY, 1978.
(2) Keller, A. *Faraday Discuss* **1995**, *101*, 1.
(3) Larionova, N. V.; Gorbacheva, N. V.; Alekseev, V. G.; Pakhomov, P. M. *Physico-Chem. Polym.* **1996**, (2), 12 (in Russian).
(4) Pakhomov, P.; Khizhnyak, S.; Kober, K.; Tshmel, A. *Eur. Polym. J.* **2001**, *37*, 623.
(5) Kober, K.; Khizhnyak, S.; Pakhomov, P.; Tshmel, A. *J. Appl. Polym. Sci.* **1999**, *72*, 1795.
(6) Snyder, R. G. *J. Chem. Phys.* **1967**, *47*, 1316.
(7) Capaccio, G.; Wilding, M. A.; Ward, I. M. *J. Polym. Sci.: Polym. Phys. Ed.* **1981**, *19*, 1489.
(8) Snyder, R. G.; Krause, S. J.; Scherer, J. R. *J. Polym. Sci.: Phys. Ed.* **1978**, *16*, 1593.
(9) Barham, P. G.; Keller, A. *J. Mater. Sci.* **1976**, *11*, 27.
(10) Davis, G. T.; Weeks, J. J.; Martin, G. M.; Eby, R. K. *J. Appl. Phys.* **1974**, *45*, 4175.
(11) Baker, A. M. E.; Windle, A. H. *Polymer* **2001**, *42*, 667.
(12) Geil, P. H. *Polymer Single Crystals*, Interscience, A Division of John Wiley & Sons: New York, 1963.
(13) Dreyfuss, P.; Keller, A. *J. Macromol. Sci.—Phys.* **1970**, *20*, 811.
(14) Dreyfuss, P.; Keller, A. *J. Polym. Sci. B.* **1970**, *8*, 253.
(15) Barham, P. G.; Keller, A. *J. Polym. Sci.: Phys. Ed.* **1989**, *27*, 1029.
(16) Rastogi, S.; Spoelstra, A. B.; Goossens, J. G. P.; Lemstra, P. J. *Macromolecules* **1997**, *30*, 7880.

MA034139G